IOP Conf. Series: Materials Science and Engineering **1301** (2024) 012138 doi:10.1088/1757-899X/1301/1/012138

# Implementation and testing of a 100 mK ADR backed by a $^4He/^3He$ sorption fridge for CMB-S4 project

**Thibault ROMAND[1,2], Alessandro SCHILLACI[1], Ahmed SOLIMAN[1], Bryan STEINBACH[1], Sofia FATIGONI[1], Thomas PROUVE[2], Jean-Louis DURAND[2], Jean-Marc DUVAL[2] and James J BOCK[1]**

[1] California Institute of Technology (Caltech), Pasadena, CA 91125, USA
[2] Univ. Grenoble Alpes, CEA/IRIG/DSBT, Grenoble 38000, France

Email: tromand@caltech.edu

**Abstract**. CMB-S4 is a ground-based experiment that will use large-format bolometer arrays to map Cosmic Microwave Background (CMB) polarization with unprecedented sensitivity, including the search for a B-mode polarization pattern associated with cosmic inflation. The focal planes on which the superconducting detectors are mounted weigh about 20 kg each and must be cooled at 100 mK. To reach this temperature for a first receiver fielding prototype hardware, we have developed an Adiabatic Demagnetization Refrigerator (ADR) used in conjunction with an existing $^4He/^3He$ sorption refrigerator.
The ADR unit described here is based on a Chromium Potassium Alum (CPA) salt pill. It is backed by a 3-stage ($^4He/^3He/^3He$) sorption fridge, coupled through a $^3He$ gas-gap heat switch. This heat switch is connected to a $^3He$ stage of the sorption fridge to dissipate the heat generated by magnetization. The ADR is cycled with a 1.3 T magnetic field. The parasitic field at the detectors' location during observations is kept below 2.5 μT thanks to a ferromagnetic shield. The pill is supported by Kevlar lines, which are doubly intercepted by the $^4He$ and $^3He$ stages of the sorption fridge to reduce conductive heat losses. With a total recycling time of 12 hours, this cryogenic assembly provides 2 μW of cooling power during 48 hours at 100 mK. The ADR has been designed by CEA/DSBT in France and is now implemented in a cryostat at Caltech.

## 1. Introduction

### *1.1. Context*

The Adiabatic Demagnetization Refrigerator (ADR) uses the magnetocaloric properties of certain paramagnetic materials to reach temperatures as low as tens of millikelvin. The heat generated while the magnetic field is increased must be dissipated by a cold bath. The ADR must then be disconnected from the bath to perform the adiabatic demagnetization that cools the material. The heat switch connecting the ADR to the bath is thus an essential part [1]. This well-known cooling technique, coupled with a helium sorption refrigerator, is a good candidate for cooling down the superconducting detectors used to observe the Cosmic Microwave Background (CMB). These Transition-Edge Sensors (TES) use the strong variation of resistance when a material is maintained at its superconducting phase transition to amplify the small temperature variation caused by the heat input of a CMB photon on the detector.

As a collaboration, this ADR has been designed and manufactured at CEA/DSBT and integrated and tested in a Caltech cryostat. This paper presents the cooling capabilities of the ADR.

### *1.2. CMB-S4 project presentation*

CMB-S4 will be the largest ground-based effort in CMB science, mapping the CMB polarization with 100 mK TES bolometers. It is a continuation of ongoing projects such as BICEP Array (Background Imaging of Cosmic Extragalactic Polarization). The ultimate goal of these experiments is measuring a specific polarization pattern (called B-mode) in the CMB radiation (the first light of our Universe). Detecting this polarized signal could validate cosmic inflation (a superluminal expansion of the Universe that theory predicts has occurred a few fractions of a second after the Big Bang) [2]. At CMB observation frequencies, the primary attenuation of the signal comes from the water vapor in Earth's atmosphere. To maximize the received signal, CMB-S4 will use 21 telescopes distributed between the South Pole Station in Antarctica and the Atacama Desert in Chile, the driest places on Earth.

The actual BICEP Array focal plane is cooled to 250 mK with a 3-stage ($^4He/^3He/^3He$) sorption fridge. CMB-S4 pSAT receiver will be a pathfinder combining the BICEP Array cryostat architecture with a new and compact ADR. This ADR will use a $^3He$ stage of the sorption cooler as a cold bath. The 100 mK temperature provided by the ADR will not only reduce the thermal noise but allow the use of new detectors. The superconducting transition of these detectors is lower than 200 mK, the physical limit of a $^3He$ sorption cooler. The ADR technology is a good candidate to reach 100 mK, particularly in terms of space requirements and ease of installation with the existing sorption fridge.

## 2. Material and methods

### *2.1. Caltech testbed*

To validate the functioning of the ADR unit, a testbed has been set up at Caltech. The cryogenic chain is composed by a Cryomech PT-415, that cools down two radiative shields to about 40 K and 4 K. A 3-stages ($^4He/^3He/^3He$) sorption fridge [3] is implemented on the 4 K plate. Its $^4He$ stage is used to condense $^3He$ of the two other stages. Its biggest $^3He$ stage (called Intermediate Cold or IC) intercepts the pumping line of the little one (called Ultra Cold or UC), reaching a temperature below 250 mK. Since the cycling of the ADR requires the dissipation of a large amount of heat during magnetization, we use the huge volume of $^3He$ in the IC stage to precool it and handle the demagnetization.

Careful work has been done to close up the 4 K area to avoid any light leakage and reduce the parasitic heat losses. Inlets are required in this enclosure to carry the current to the ADR magnet and read temperatures, for example. Each hole has been closed with a flange and reinforced with aluminum tape. In addition, the side panels that close the 4 K area have been painted with “Bock Black”, a carbon-loaded Stycast coating that increases the exchange surface and absorb any light that may enter [4]. Moreover, every measurement wire that goes to 100 mK has been carefully thermalized at 4 K, 1 K, and 300 mK. Wire length has been maximized to decrease the conduction heat input. We use manganin wires. Finally, a magnetometer has been implemented in the cryostat to measure the stray field at the detector’s location.

### *2.2. Specificities of the ADR unit*

The ADR presented here is made of a CPA (Chromium Potassium Alum, $CrK(SO_4)_2\cdot 12(H_2O)$) pill. The net weight of our pill is 226 g for a volume of 137 cm$^3$. The calculated density is a bit lower than the published value of 1.83 g/cm$^3$ because of the non-perfect growth of the salt pill around the copper wires. The ADR cold finger is a copper piece crimped to a thermal bus around which the CPA crystal has grown. This assembly is connected to the ADR shield through 16 low thermal conductivity Kevlar supports, as shown in Figure 1 below. Each of these lines is doubly intercepted with copper wires: at 1 K by the $^4He$ stage of the sorption and at 300 mK by its IC $^3He$ stage. A superconducting Niobium-Titanium (Nb-Ti) coil is placed around the pill without touching it. This coil needs a 6 Amps current input to reach the nominal 1.3 T magnetic field. The current is carried in 3 mm-thick Brass leads through the cryostat to the 50 K plate, then in a ReBCO (Rare-earth Barium Copper Oxide) tape to the 4 K plate, and finally in 300 μm-thick superconducting Nb-Ti leads to the magnet itself. The magnet is quench-protected by a diode circuit. The body of the ADR consists of a ferromagnetic passive shield that allows condensing of the field lines to reduce the parasitic field around the ADR.

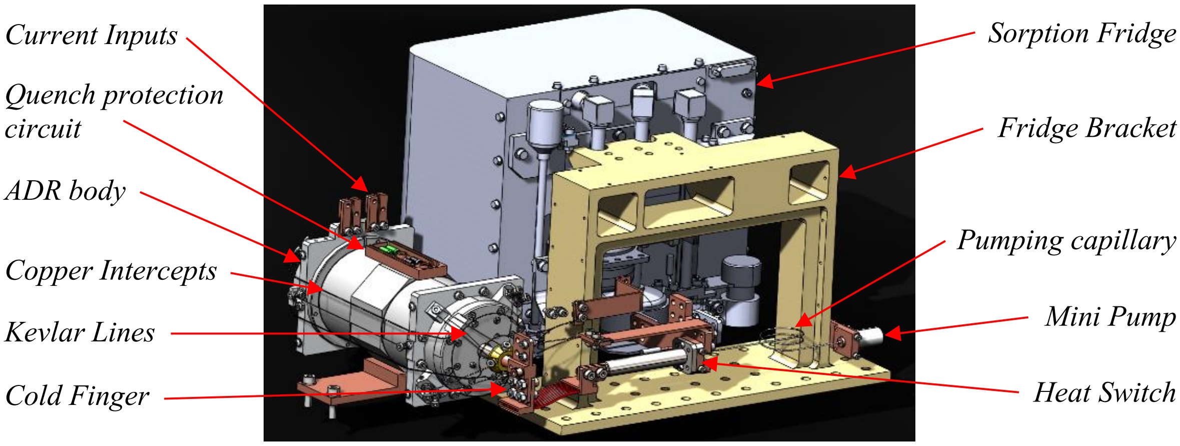


**Figure 1.** 3D model of the ADR connected to the sorption fridge.

The ADR is connected to the sorption IC stage through an active gas-gap $^3$He heat switch (HS), as shown in Figure 1 above. To open and close the switch, one can control the amount of $^3$He gas in it thanks to a mini pump. The activated charcoal cylinder in the pump absorbs gas when cooled and releases gas when heated. When no gas is present in the switch, both ends not being in contact, the ADR is disconnected from the sorption fridge (the HS is open). Once the mini pump is heated, gas is released in the switch and connects the ADR to the sorption fridge (the HS is closed). Since the mini pump must be heated to control gas adsorption, it has been remoted to 4 K to avoid heat input to IC at 300 mK. It is connected to the HS body by a 0.6 x 0.8 mm Stainless Steel pumping capillary.

### *2.3. ADR cycling time*

The ADR presented in this paper aims to maintain CMB-S4 detectors at 100 mK for 48 hours of observation. It is important to reduce the cycling time to maximize the observation periods. The actual sorption fridge can maintain the focal plane at 250 mK for 48 hours with a 8-hours cycling time (for a double $^4$He cycling). Since the ADR is connected in series with the sorption IC stage, the cycling of the ADR must be synchronized with the sorption fridge. The ADR recycling phase consists in increasing the magnet current to 6 A, with a closed HS to evacuate the heat produced towards IC, and then opening the HS to perform adiabatic demagnetization. The regulation phase follows, gradually reducing the current to maintain the temperature at 100 mK until the magnet is fully demagnetized.

As a first test, the ADR has been cycled after the completion of the sorption fridge cycle. The heat generated during the magnetization has been slowly ejected toward IC by regulating the ADR temperature at 500 mK, as shown in Figure 2 below (left). The demagnetization has been handled after the HS opening and stabilization at IC base temperature (270 mK). This cycle took about 10 hours (5 hours for the magnetization and 5 hours for the stabilization), in addition to the 8-hours sorption fridge cycle. Eighteen hours of cycling time is too long for a 48-hour observation period.

To reduce the overall cycling time, the ADR has been magnetized during the sorption fridge cycle. This one has been modified in order not to exceed the critical temperature at which the Nb-Ti current leads become non-superconductive (9.3 K), to avoid quenching them if energized. In the previous configuration, the cold plate was warming to about 10 K when the hot pumps were connected to it. Though the risk of transiting the Nb-Ti to its normal state is low, we decided to pause the closing of the sorption pump's heat switches to maintain nominal operation. This pause connects them progressively to the cold plate and slowly dissipates the heat toward the Pulse Tube. The cold plate temperature doesn't exceed 7 K in these conditions. Another concern is that the IC must cool an energized ADR pill, which has a big heat capacity in these conditions. The significant enthalpy of the IC stage (filled with 20 STP liters, or 0.88 moles of $^3$He) can handle it. Once the IC reaches its base temperature of 270 mK, the HS is opened, and the ADR is demagnetized. Figure 2 below shows a comparison of the two described cycles. When the ADR is cycled during the sorption fridge cycle, the global cycling time is **12 hours**. During the demagnetization phase, the current decreases with a ramp rate of 0.5 A/min.

IOP Conf. Series: Materials Science and Engineering **1301** (2024) 012138 doi:10.1088/1757-899X/1301/1/012138

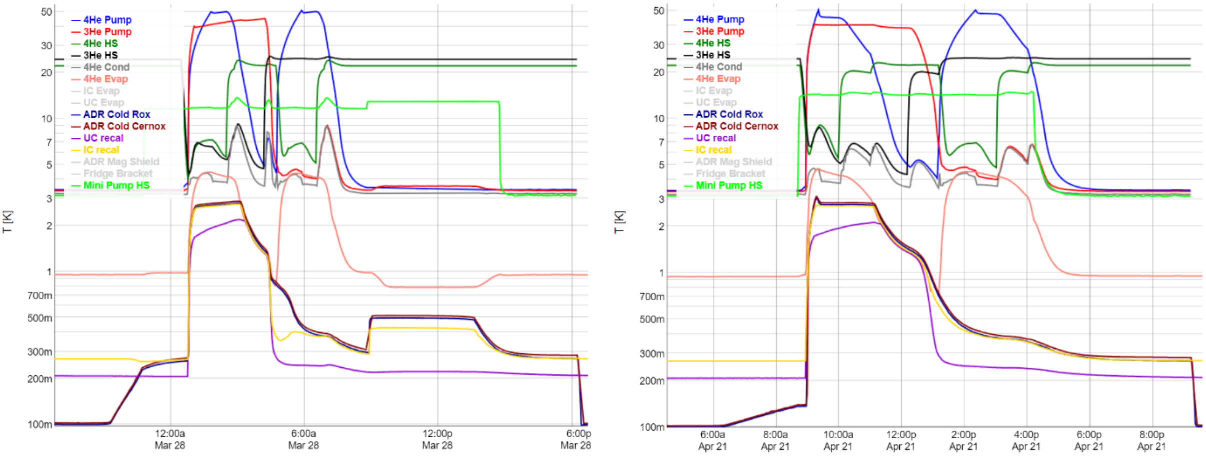


**Figure 2.** Comparison of the ADR cycling after (left) and during (right) the sorption fridge cycle.

## 2.4. *Pill's entropy graphs*

The CPA pill entropy has been calculated using equation (1) below, admitted from [5].

$$S(B,T) = \mathrm{R} \cdot \ln\left\{\frac{\sinh[x(2J+1)/2]}{\sinh(x/2)}\right\} + \frac{x}{2}\left\{\coth\left(\frac{x}{2}\right) - (2J+1)\cdot\coth\left[\frac{x(2J+1)}{2}\right]\right\} \quad (1)$$

$$\text{with} \quad x = \frac{g\mu_\mathrm{B}\sqrt{B^2+{b_\mathrm{i}}^2}}{\mathrm{k_B}T} \quad (2)$$

With $S$ the entropy (J/K), $B$ the magnetic field applied to the pill (T), $T$ the temperature of the pill (K), R the universal gas constant (8.31 J/mol/K), $J$ the total angular momentum quantum number (3/2 for CPA), $g$ the Landé factor (1.98 for CPA), $\mu_\mathrm{B}$ the Bohr magneton ($9.27\cdot10^{-24}$ J/T), $b_\mathrm{i}$ the internal field (0.01 T for CPA), and $\mathrm{k_B}$ the Boltzmann constant ($1.38\cdot10^{-23}$ J/K). To have the entropy in J/K units, we used the molar mass of CPA (499.4 g/mol), and the mass of our CPA pill (226 g).

Figure 3 below shows the entropy as a function of (left) the pill's temperature and (right) the magnetic field applied to it. An ADR cycle is plotted on each graph. At (1) the ADR is at IC base temperature (270 mK) and the pill's entropy is 5.22 J/K. The sorption fridge cycle starts with a closed HS and brings the ADR temperature to about 3 K (2). The magnet current is increased to 6 A while the heat generated by this magnetization is rejected to IC (3). The sorption fridge cycle brings the IC and the ADR temperature to 270 mK with a 1.3 T magnetic field. The entropy of the pill decreases, and the energy is rejected toward IC (4). After opening the HS, the ADR is demagnetized to about 0.45 T. Since this demagnetization is adiabatic, the pill's temperature drops to 100 mK (5). The residual field is then slowly decreased to regulate this temperature at 100 mK until the magnet is fully demagnetized (6). The pill's entropy increases to keep the ADR cold finger at 100 mK. The ADR temperature finally increases under the effect of the parasitic heat losses, until it stabilizes at IC's temperature (1). The HS can be closed, and the ADR recycled.

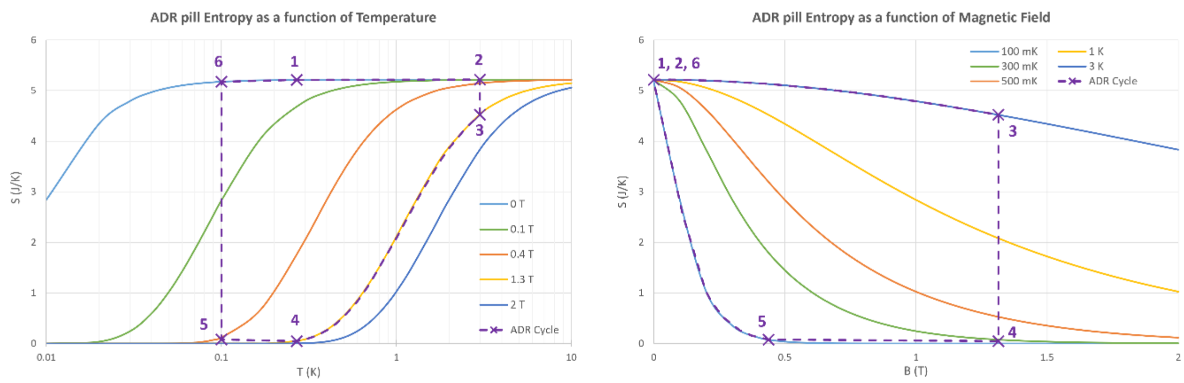


**Figure 3.** ADR pill entropy graphs with cycle representation.

IOP Conf. Series: Materials Science and Engineering **1301** (2024) 012138 doi:10.1088/1757-899X/1301/1/012138

## 3. Results and discussions

### *3.1. Parasitic heat losses*

The parasitic heat losses correspond to the sum of all unwanted power inputs that reach the cold part of the ADR. This background power is mainly due to radiation and conduction since the cryostat is under vacuum. The radiation comes from the hot surfaces surrounding the ADR; one wants to reduce the temperature of these surfaces to decrease the parasitic heat losses. Conduction occurs mainly through the HS, the Kevlar lines, and the measuring wires (we have two thermometers and one heater on the ADR cold finger). The power input from IC through the open HS has been calculated to be 250 nW. Thanks to the dual intercept in the Kevlar lines (at 1 K and 300 mK), the estimated power input through them is roughly 50 nW. The input through the measuring wires is negligible since they are thermalized at IC temperature and have a very low thermal conductivity.

The parasitic heat losses are experimentally measured using two methods:

- The first one lets the ADR's temperature drift without any current in the magnet. The temperature rise is fully due to parasitic losses. To find out what power corresponds to the slope of the curve $T = f(t)$, a known power is applied. Once this power is removed, the temperature again rises solely due to parasitic losses. The background power is calculated by comparing the slopes with and without the known applied power. This protocol can be done at different temperatures.

- The second method compares different hold time runs and uses equation (3), explained further below, to access the background power. This method supplies parasitic heat losses only at the regulation temperature (usually 100 mK).

During the first test of the ADR, the measured background power was more than 2 µW, and the hold time didn't satisfy the requirement of 48 hours at 100 mK. Since the estimated conductive power is around 0.3 µW, the hypothesis that the additional 1.7 µW heat input comes from radiation has been put forward. Careful work closing all the light leaks in the 4 K area has thus been carried out. The parasitic heat losses have been measured as a function of the ADR cold finger temperature using the first method. Results are plotted in Figure 4 below.

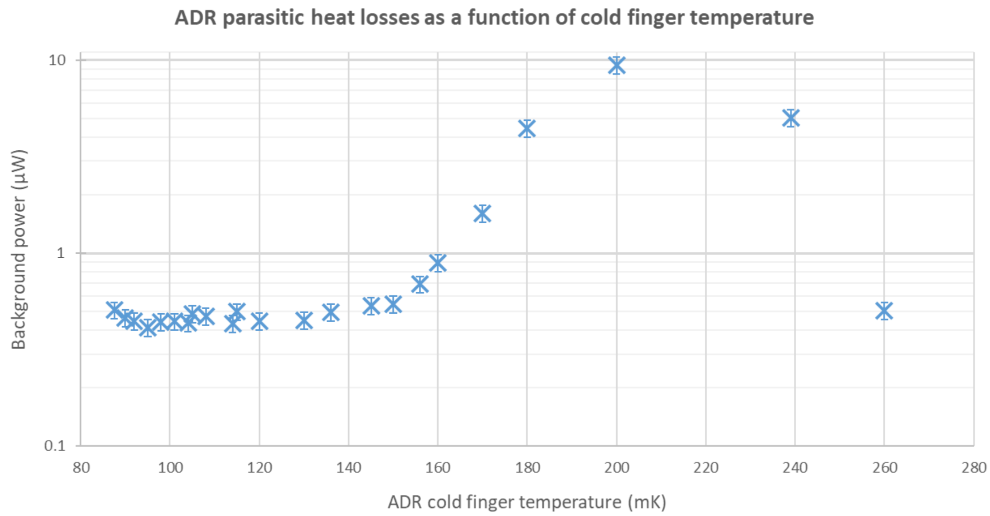


**Figure 4.** Parasitic heat losses measurements.

Figure 4 above shows that the background power around 100 mK has been decreased to **0.45 ± 0.02 µW**. We believe it is equally divided between radiation and conduction. The parasitic heat losses increase when the ADR temperature reaches 150 mK. This is most likely due to liquid $^3$He presence in the gas-gap HS, which connects the ADR to the IC stage of the sorption fridge. Below 150 mK, the saturation vapor pressure of $^3$He is so low that the heat input is negligible even if liquid $^3$He is present in the HS. As the ADR temperature goes up, the background power increases until it reaches 10 µW at 200 mK. Above this temperature, the ADR and IC temperatures are getting closer, and the parasitic heat input through the HS is less significant. Once the ADR stabilizes at IC temperature (270 mK), the background power measured with this method is null since ADR is connected to IC and it actively regulates the temperature by evaporating liquid $^3$He. Therefore, the veracity of our results when ADR starts to be connected to IC can be debated. As liquid $^3$He is present in the HS, the switch becomes useless between 170 mK and 400 mK; it is closed regardless of its mini pump temperature.

### *3.2. ADR pill characterization*

To characterize the CPA pill developed for this ADR, several hold time runs have been carried out by applying a known power to the ADR cold finger. The time during which its temperature can be regulated at 100 mK (until the magnetic field is exhausted) corresponds to the hold time. To determine the maximal hold time, a similar test has been realized without any applied power (letting the magnetic field decrease under the only effect of the background power). In these conditions, the ADR stayed at 100 mK for about 208 hours (more than a week). The sorption fridge IC stage stayed at its base temperature (270 mK) for the entire run. However, its $^4$He stage ran out of liquid after 190 hours. The temperature jumped to 2.3 K (instead of 950 mK), increasing the parasitic heat losses reaching the ADR cold finger through the Kevlar lines. Thanks to these runs, the internal energy of the pill can be calculated using equation (3) below, with $E$ the energy (J), $t_0$ the hold time without any applied power, $P_0$ the background power, and $t_1$ the hold time with a $P_1$ applied power.

$$E = t_0 \cdot P_0 = t_1 \cdot (P_1 + P_0) \quad (3)$$

Figure 5 below shows the hold time as a function of applied power and presents how the pill's remaining energy decreases as the magnet's current is lowered. The pill's remaining energy at the maximal magnetic field after demagnetization to 100 mK (0.45 T) is assimilated to its internal energy at this temperature. Comparing the hold times using equation (3), our pill's internal energy at 100 mK is **0.336 ± 0.004 J**. The left plot shows that the hold time of the ADR with 1.5 µW of applied power is around 48 hours. Since the background power is 0.45 µW, the global cooling power that this ADR can provide for 48 hours of observations at 100 mK is about 2 µW (0.338 J), in-line with our expectations.

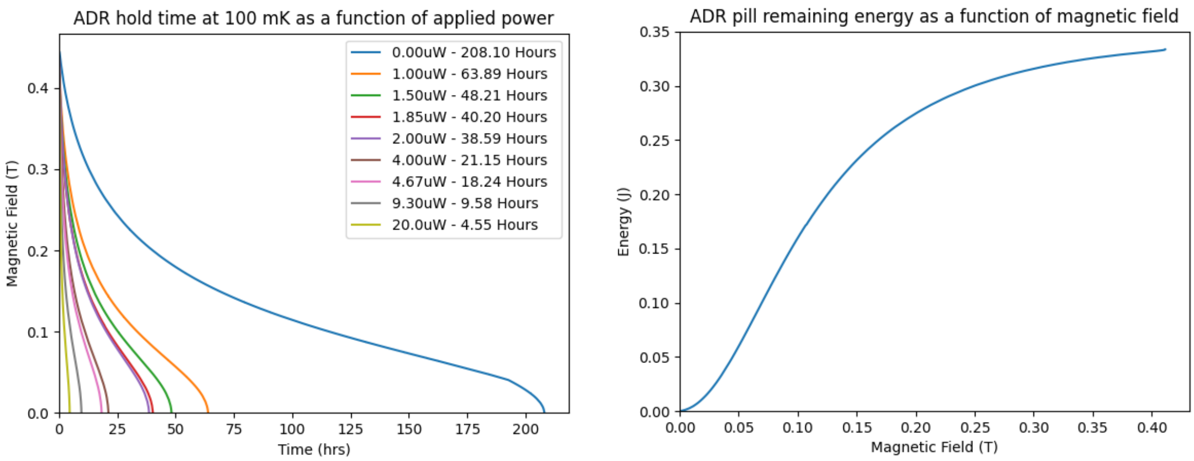


**Figure 5.** ADR hold time (left) and remaining energy (right) measurements.

Additionally, the conductance between the pill and the ADR cold finger has been measured using the first method described in 3.1. To access it, we measure the temperature drop when the known power on the cold finger is suddenly removed. The cold finger temperature goes down because the pill's temperature stayed colder. This conductance describes how well the pill is connected to the thermal bus of the ADR cold finger. At 100 mK, the measured conductance is **5.9 ± 0.3 µW/mK**. In other words, if the ADR cold finger is regulated at 100 mK with 2 µW of power reaching it, the pill temperature is about 99.7 mK. This conductance increases as the ADR temperature goes up, which means that the pill and the cold finger are becoming better thermally connected as temperature increases.

Finally, the heat capacity ($C_p$) of our CPA pill has been measured using the same method [1]. The temperature rise has been measured for different applied energies. The applied energy is the sum of the applied power and the background power multiplied by the time it is applied. Figure 6 below shows our pill's $C_p$ as a function of its temperature. The theoretical plot has been extracted from [6].

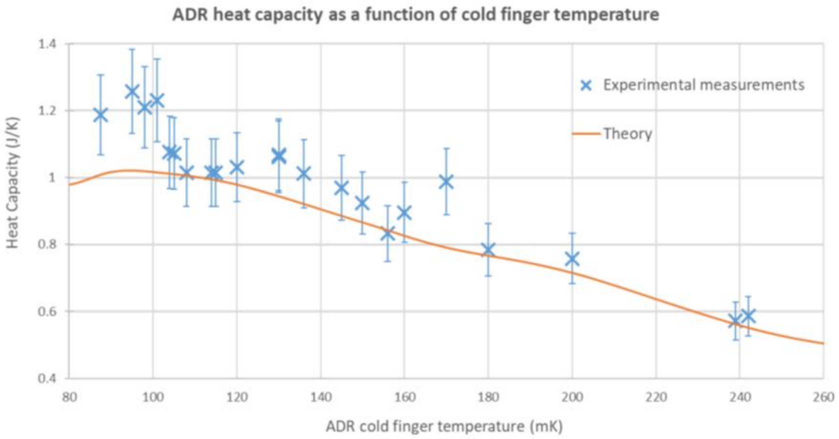


**Figure 6.** CPA pill heat capacity measurements.

Around 100 mK, we measured our CPA pill's heat capacity to be **1.0 ± 0.1 J/K**. Its specific heat capacity is around 4.4 J/K/kg, and its volumetric heat capacity is around 0.0073 J/K/cm$^3$, given the mass and volume of this pill. Above 100 mK, the CPA heat capacity decreases when its temperature grows. Our measurements are consistent with the theory given in [6].

### *3.3. Parasitic magnetic field*

The detectors used to observe the CMB (and their amplification circuit) are extremely sensitive to the magnetic field. The ADR described here is meant to cool these detectors at 100 mK, but requires a 1.3 T magnetic field. To concentrate the field lines and prevent them from spreading outside the ADR's body, its magnet is surrounded by a magnetic shield. The one designed for this ADR is passive and is made of a thermally treated ferromagnetic material, then nickel-plated to protect against oxidation. In addition, the detectors and their amplification circuit are enveloped in a superconductive Niobium shield.

A measurement campaign has been carried out to determine the parasitic magnetic field during ADR cycling. Two Bartington fluxgate magnetometers have been used. The first one is located inside the cryostat, at 4 K, about 20 cm from the magnet center, centered and coaxial with it. The second one is outside the cryostat and is free to move around it. Figure 7 below shows the parasitic field measured by these two sensors as a function of the current injected in the ADR's magnet. The outside sensor has been put at 30 cm from the ADR for this campaign.

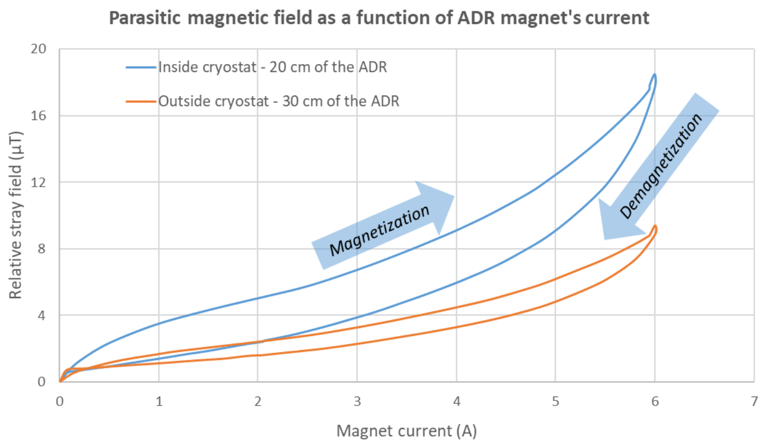


**Figure 7.** Parasitic magnetic field around the ADR.

The graph shows the relative field, i.e., the measured field at which the earth's magnetic field (measured beforehand) has been substituted. Figure 7 above shows that the maximal relative parasitic field during ADR cycling (when its magnet is powered with 6 A) is 18 µT at 20 cm of the ADR magnet and roughly 10 µT at 30 cm of it. A magnetic screening simulation gives 40 µT at 20 cm and 14 µT at 30 cm, with 6 A in the coil (1.3 T in the center of the magnet). This simulation is a bit pessimistic, but the discrepancies with experimental measurements are mainly due to uncertainties in the magnetic properties of the ferromagnetic shield.

One can see a hysteresis behavior between magnetization and demagnetization since the magnetic shield is made with a ferromagnetic material. During observations, the maximal current in the magnet is 2 A (0.45 T) after demagnetization to 100 mK. In these conditions, the parasitic field is around **2.5 ± 0.2 µT** at the detector's location. This value is much lower than Earth's magnetic field (around 50 µT), but reaches directly the detectors, while Earth's magnetic field can be screened. Precautions must therefore be taken to prevent ADR parasitic magnetic field from interfering with the detectors.

## 4. Conclusion

This paper presents the performances of an ADR unit designed by CEA/DSBT for CMB-S4 project. Implemented in a testbed at Caltech and backed by a $^4He/^3He/^3He$ sorption fridge, this ADR can provide 2 µW of cooling power at 100 mK for 48 hours of observation. The internal energy of the CPA pill manufactured for this ADR is about 0.34 J. The ADR is cycled in parallel with the sorption fridge and the ratio observation/cycling is 4. The parasitic heat losses reaching the ADR cold finger in these conditions have been decreased to 0.45 µW. These losses can be higher with a real focal plane and all the optics necessary for observations [7]. Thanks to a passive magnetic shield, the parasitic field during observations is kept below 2.5 µT at the detector's location.

After validating that this ADR can cool down a focal plane to 100 mK, new detectors will be tested for CMB-S4 project. A first pathfinder telescope will use the same architecture as BICEP Array, to which the ADR will be added. The purpose of this pathfinder is to run the detectors and optics developed for CMB-S4 and show that they can control systematic errors sufficiently as an early test for CMB-S4. The relative ease of installation of the ADR cooler makes possible a quick validation in a constrained cryostat environment. Once the operation of the detectors will be proven on this ADR-based pathfinder, a Dilution Fridge will be preferred to cool them on a larger scale telescope.

## 5. References

[1] Luchier N, Duval JM, Duband L and Tirolien T 2012 Performances of the 50 mk adr/sorption cooler *Cryogenics* vol 52 (4-6) pp 152-157
[2] BICEP/Keck Collaboration: Ade PAR et al. 2022 The latest constraints on inflationary b-modes from the bicep/keck telescopes *Preprint* 2203.16556
[3] Duband L, Prouvé T, Bock J, Moncelsi L and Schillaci A 2020 Sub-kelvin cooling for the bicep array project *Proc. Int. Cryocooler Conf. (Burlington, 2018)* vol 20 p 387
[4] Bock J 1994 Rocket-borne observation of singly ionized carbon 158 um emission from the diffuse interstellar medium *Ph.D. Thesis (University of California, Berkeley)*
[5] Pobell F 1996 Refrigeration by adiabatic demagnetization of a paramagnetic salt *Matter and Methods at Low Temperatures* pp 169-180
[6] Vilches OE and Wheatley JC 1966 Measurements of the specific heats of three magnetic salts at low temperatures *Physical Review* vol 148 (2) p 509
[7] Goldfinger D et al. 2022 Thermal testing for cryogenic cmb instrument optical design *Proc. SPIE Millimeter, Submillimeter, and Far-Infrared Detectors and Instrumentation for Astronomy XI* vol 12190 pp 805-813

**Acknowledgments**
We thank Florian BANCEL for the design of the ADR and Heat Switch package. We thank the SHEREx team for lending the Caltech test cryostat.